Characterization of superconducting nanometric multilayer samples for superconducting rf applications: First evidence of magnetic screening effect

C. Z. Antoine,[1] S. Berry,[1] S. Bouat,[2] J-F. Jacquot,[2] J-C. Villegier,[2] G. Lamura,[3] and A Gurevich[4]

[1]*CEA, Irfu, SACM, Centre d'Etudes de Saclay, 91191 Gif-sur-Yvette Cedex, France*
[2]*CEA, Inac, 17 Rue des Martyrs, 38054 Grenoble-Cedex-9, France*
[3]*LAMIA, Physics Departement, Genoa University Via Dodecaneso 33, 14146 Genova, Italy*
[4]*National High Magnetic Laboratory, Florida State University, 1800 E. Paul Dirac Drive, Tallahassee, Florida 32310, USA*

(Received 30 November 2009; published 3 December 2010)

The best rf bulk niobium accelerating cavities have nearly reached their ultimate limits at rf equatorial magnetic field $H \approx 200$ mT close to the thermodynamic critical field H_c. In 2006 Gurevich proposed to use nanoscale layers of superconducting materials with high values of $H_c > H_c{}^{\mathrm{Nb}}$ for magnetic shielding of bulk niobium to increase the breakdown magnetic field of superconducting rf cavities. Depositing good quality layers inside a whole cavity is rather difficult, so as a first step, characterization of single layer coating and multilayers was conducted on high quality sputtered samples by applying the technique used for the preparation of superconducting electronics circuits. The samples were characterized by x-ray reflectivity, dc resistivity (PPMS), and dc magnetization (SQUID) measurements. Dc magnetization curves of a 250 nm thick Nb film have been measured, with and without a magnetron sputtered coating of a single or multiple stack of 15 nm MgO and 25 nm NbN layers. The Nb samples with/without the coating exhibit different behaviors and clearly show an enhancement of the magnetic penetration field. Because SQUID measurements are influenced by edge and shape effects, we propose to develop a specific local magnetic measurement of H_{C1} based on ac third harmonic analysis in order to reveal the true screening effect of multilayers.

DOI: 10.1103/PhysRevSTAB.13.121001 PACS numbers: 29.20.−c, 74.78.−w, 85.25.Am

I. INTRODUCTION

Bulk niobium cavities have proven to provide the highest accelerating gradients up to 40 MV/m in superconducting rf cavities for particle accelerator applications. When the accelerating field reaches this value, the magnetic field component near the equator is close to the thermodynamic critical field $H_c{}^{\mathrm{Nb}} \approx 200$ mT at which the screening current density reaches the maximum depairing current density in a superconductor.

There are several evidences that the rf dissipation observed in Nb cavities at high field has a magnetic origin, in which case the BCS surface resistance R_{BCS} increases at high field. As H_{rf} approaches H_C, the normal electron density and R_{BCS} increases due to the effect of the rf current pair breaking on thermal activation which in turn increases heating, making R_{BCS} nonlinear at high field. So far, this nonlinear rf response has only been evaluated for type II superconductors in the clean limit and at low frequency. It shows that at high field the surface resistance $R_s\,(T, H_{\mathrm{rf}})$ increases exponentially with field and temperature, and can give rise to thermal runaway [1,2].

This model could, in particular, explain the hot spots observed on cavities where either surface defects or bundles of trapped vortices can produce localized dissipative regions from which heat spreads along the cavity surface over tens of mm. The magnetic/vortex origin of some of such hot spots has been recently demonstrated [3].

The necessity to prevent strong rf dissipation due to vortex penetration at high fields has resulted in the monopoly of niobium in superconducting rf applications since the clean Nb has the highest value of the lower critical field $H_{C1} \approx 180$ mT at 0 K among all superconductors. Attempts to use higher T_C and H_{C2} superconductors have failed so far, probably due to their low H_{C1}, which allows early penetration of magnetic vortices resulting in high surface dissipation (for a recent review on that topic, see [4]).

II. MULTILAYERS

The use of composite structures comprised of nanoscale multilayers of superconducting materials with $H_C \gg H_C^{\mathrm{Nb}}$ for magnetic shielding of niobium cavities has been proposed to significantly increase the breakdown field in rf accelerating applications [5].

Very high H_{C1} can indeed be achieved with films whose thickness d is smaller than the magnetic penetration depth λ, in a configuration where the field is parallel to the surface of the film [5]. So such films could be used to screen bulk niobium and allow a much higher field to be reached inside the cavities. Bulk niobium is still necessary to prevent perpendicular vortices to penetrate the film and dielectric layers are needed to prevent Josephson coupling between coating layers and the Nb substrate. Such structures would be particularly efficient in the case of rf elliptic cavities where the magnetic field is confined in the cavity and is parallel to its surface.

Deposition techniques

Thin film deposition on curved, large surfaces like the cavities is difficult as has been shown recently (see e.g. [6]). Thus, we are searching for a deposition technique which can then be developed for cavity geometries to provide uniform coating of nanolayers, with sharp interfaces, low densities of defects, including grains boundaries and impurities, and low residual stress. Testing such nanostructures deposited inside cavities would be fairly easy since in this field configuration no side effects are expected.

As a first step, we have prepared high quality samples and characterized those using standard measurements. Several deposition techniques can achieve very good quality films in specific conditions, but their characterization using classical dc techniques cannot be unambiguously extrapolated to predict the rf behavior of the film coating in a cavity. Nevertheless, demonstrating the effective screening effect of nanometer scale NbN films (high H_{C1}) on good Nb samples could initiate the interest of the scientific community in searching alternative deposition techniques like the one presented in [7,8]. To reach this goal, the evaluation of the first penetration field for layered samples as compared to the bulk niobium is of fundamental importance.

In order to produce high quality layered films, we applied the magnetron sputtering technique, an asserted technique well developed for the preparation of superconducting electronics circuits particularly for Josephson junctions and detector fabrication.

III. EXPERIMENTAL DETAILS

We have grown one 25 nm single NbN layer (SL), and one multilayer (ML) with four 12 nm NbN layers deposited on a 250 nm Nb layer. The intermediate dielectric layer was MgO (all parameters of the samples are listed in Table I). NbN layers were deposited by dc magnetron sputtering from a six-inches diameter niobium target in a reactive (nitrogen/argon) gas mixture at 300°C. The same target is used for Nb deposition applying only argon pressure, whereas the MgO layer is rf-magnetron sputtered from an MgO target. More details on the technique can be found in [9]. The NbN top layer is further reactive ion etched on a part of the wafer to provide the bulk niobium reference sample (Ref).

A. X-ray characterization

High angle x-ray diffraction measurements provide information about the crystalline relations between the substrate and the deposited layers. For instance, for sample SL we observed that Nb, NbN, and MgO were all (200) textured at 100% although it was not possible to determine if they were polycrystalline or monocrystalline. In addition, the NbN layer was slightly expanded (0.5%) in the (200) direction. For sample ML we observed also a (200) texture for each layer, but the (200) Nb texture is only partial (~ 89%).

Low angle x-ray reflectivity gave information about thicknesses and interface roughness of the different layers. The measured signal was fitted using Paratt formalism that takes into account the existence of several layers of various electronic densities [10]. The resulting data are summarized in Table I.

B. T_C measurements

The superconducting critical temperature T_c of each sample was measured using a quantum design PPMS facility. Measurements of the resistive transition (Fig. 1) show that ML exhibits a higher $T_c = 15.4$ K than the 250 nm Nb substrate layer (Ref, $T_c = 8.9$ K) but lower than SL ($T_c = 16.4$ K). T_c values of NbN films, close to the bulk $T_c = 17$ K of NbN, indicate good quality of the films.

C. SQUID measurements

Samples for SQUID measurements were cut to $5 \times 5\ \mathrm{mm}^2$ and glued to high purity quartz wires and aligned either parallel or perpendicular to the magnetic field. The dc magnetization curves M(H) parallel to the film surface have been measured using a quantum design MPMS equipped with a setup which enables simultaneous measurements of M(H) for both transverse and longitudinal

TABLE I. Summary of the x-ray reflectivity analysis.

Sample SL	Thickness (nm)	Roughness (nm)	Sample ML[a]	Thickness (nm)	Roughness (nm)
Nb	250	1	Nb	250	1
MgO	14	1	MgO	15	1
NbN	25	1.5	NbN	12	1.5

[a]Sample ML has four NbN/MgO layers of the same thickness.

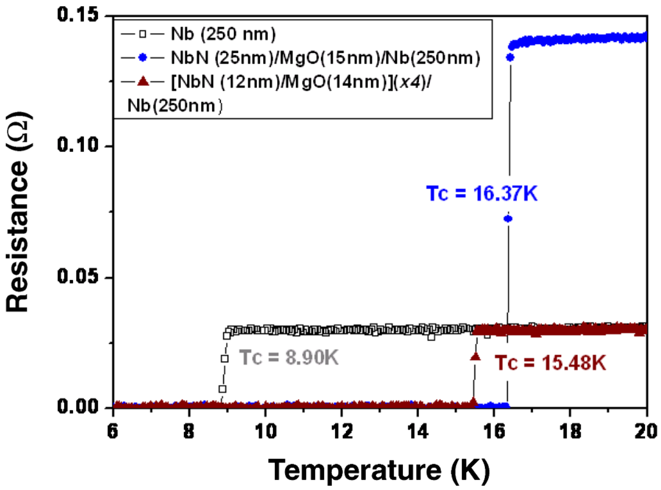

FIG. 1. Resistive transition of an Nb film covered or not by a NbN/MgO multilayer.

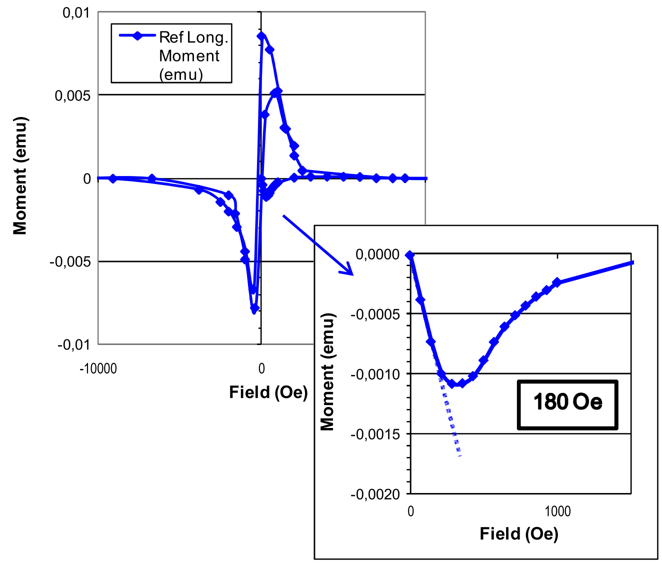

FIG. 3. Magnetization curves at 4.5 K for the reference sample (250 nm Nb): longitudinal moment. The inset shows the determination of the first penetration field B_P. As expected for an isotropic superconductor, B_P is found the same in the transverse direction (not shown here).

moment orientation. The orthogonal field configuration was also tested.

Note that H_{C1} extracted from dc measurements is lower than H_{C1} at rf frequencies. Generally H_{C1} (unlike the superheating field) increases as the frequency increases because the vortex does not have enough time to hop over the magnetic surface barrier.

SQUID measurement of thin superconducting films with H parallel to the sample plane is fairly difficult to analyze as has been pointed out in numerous publications (see e.g. [11–22]).

First of all, we detected a strong transverse magnetization signal in all the samples, over a wide range of fields, which induced some cross talk in the longitudinal detection loop (as sketched in Fig. 2). The transverse component should not be observed in the film in the Meissner state in a parallel field [16,17], but with a ratio aspect of 20 000 characteristic of our samples, any small misalignment between the field and the sample surface ($> 0.005°$) will induce a small perpendicular component of the magnetic moment [13]. Because of the large demagnetization factor, this small perpendicular field component can also cause penetration of vortices perpendicular to the film surface and induce a remnant transverse moment. The purely geometrical origin of this effect has been inferred by noting that the first penetration field (not shown) extracted by the transversal component is always the same for SL, ML, single Nb, or a single NbN layer. However, the longitudinal component of the magnetization for the parallel field configuration shows a clear enhancement of the first penetration field (see Fig. 3), even though only one side of our Nb film was covered with NbN layers.

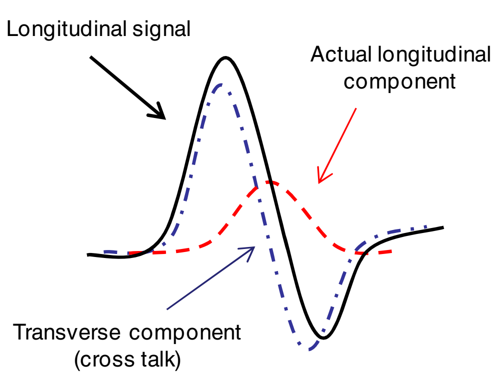

FIG. 2. Schematic feature of SQUID signals before and after deconvolution.

D. Signal analysis

If the magnetic barycenter of the sample was perfectly centered on the detection coils symmetry axis, there would be no SQUID response cross talk between the longitudinal and the transverse magnetic moment [23]. As this condition is practically impossible to achieve, we have processed the SQUID raw data to extract separately the longitudinal and transverse magnetic moment. The commercial fitting procedure is not able to fit properly such a composite signal and we had to develop a proper *ad hoc* procedure to extract the true longitudinal response.

This procedure was performed in three steps: first, we apply a Fourier transform (FFT) on the SQUID raw data in order to separate the symmetric (even) signal from the asymmetric signal (odd). Once the separation of the two signal is done, we perform back an inverse Fourier transform of the real part of the result. Finally, we apply an iterative fit with the appropriate SQUID response equation for each set of coils. This last step is similar to the usual commercial fitting procedure.

The paramagnetic signal of the sapphire substrate was measured independently and then subtracted from the data.

Note that qualitative conclusions drawn from the untreated signal (as previously published [24]) are overall not changed, but in fact they reflected only the transverse component. The general feature of the longitudinal moment is now totally changed as it was dominated by the transverse signal cross talk.

For the sake of simplicity, we will only present the results for the reference R and the single NbN layer SL in this section. The multilayer presents the same general features as SL, but with additional instabilities in the first and third quadrant (probably due to vortex jump instabilities during the field change [25,26]), which will be detailed elsewhere.

Figure 3 shows the longitudinal component of the moment of the reference sample (250 nm Nb) measured at $T = 4.5$ K. The first penetration field of about 18 mT for the Nb reference sample is much lower than the $B_{C1} \sim 150$ mT at 4.5 K for clean bulk Nb, but is consistent with the penetration fields of magnetron sputtered films, where values around 10 mT have been observed [27].

Figure 4 shows the magnetization curve for the SL samples (25 nm NbN layer). In this case the longitudinal moment exhibits a totally different behavior: it has a fish-tail shape commonly observed on thin plate type II superconductors [25,28–30].

The first penetration field in the longitudinal direction is greatly enhanced and reaches 960 Oe, ~5 times higher than that of the reference.

We have also measured under the same conditions a single (~ 30 nm) layer of NbN deposited on sapphire without Nb underneath. As shown on Fig. 5, in this case the longitudinal magnetization curve exhibits a first penetration field B_P, about 18 mT. The magnetization curves

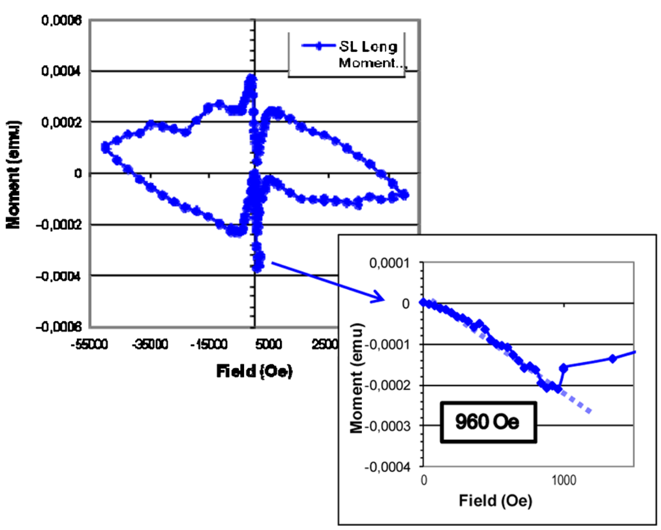

FIG. 4. Magnetization curves at 4.5 K for the SL sample (25 nm NbN top layer): longitudinal moment. The inset shows the determination of the first penetration field B_P.

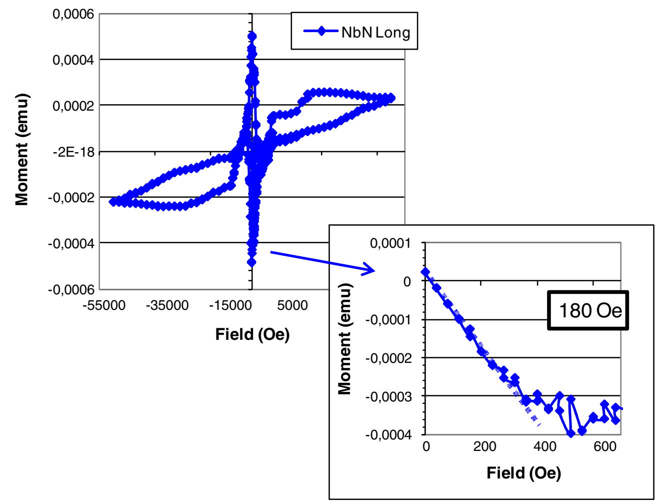

FIG. 5. Magnetization curves for a NbN sample (~ 30 nm NbN directly deposited on sapphire): longitudinal moment. The inset shows the determination of the first penetration field B_P.

also exhibit a larger hysteresis (between −5000 and +5000 Oe) in the longitudinal as well as in the transverse direction (not shown), which is not observed on the SL layer. This observation and the results presented in the next section support that the enhanced first penetration field observed on SL is related to the whole multilayer structure rather than the thin NbN layer alone. In this case the Nb substrate provides an effective barrier for penetration of perpendicular vortices in NbN film.

IV. PERSPECTIVES

A. 3rd harmonic analysis

Since SQUID measurements are strongly influenced by the film orientation, edge, and shape effects, we propose to

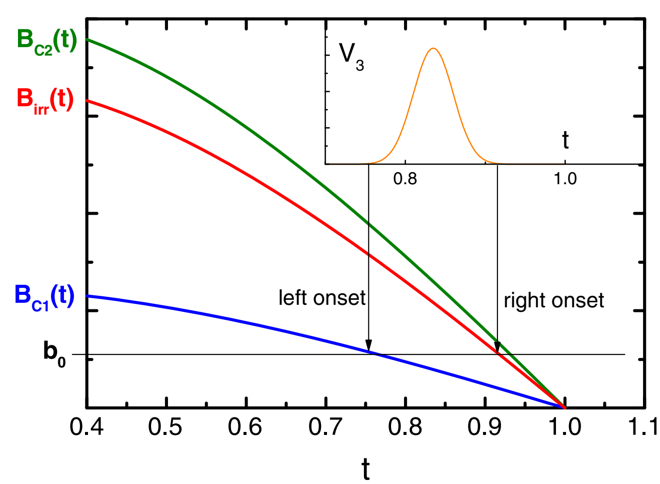

FIG. 6. Principle of third harmonic analysis (see text for details). $t = T/T_C$.

develop a specific local magnetic measurement of H_{C1} based on ac third harmonic analysis as described in Ref. [31]. This technique is based on the hysteretic behavior of the magnetization in the critical state, which gives rise to nonzero odd harmonics in the spectrum of the electrodynamic response of superconductors exposed to an ac magnetic field. In Fig. 6, $V_3(T)$ is strictly equal to zero in the Meissner phase, but it acquires finite values with a bell-shaped temperature dependence in the mixed state below the irreversibility line, and it comes back to zero in the flux flow and normal state regimes.

The first measurement on 80 nm niobium multilayers seems to show a clear increase of B_{C1} in perpendicular field configuration [31]. Likewise, our samples were also measured in the perpendicular field. The behavior of the samples SL is clearly different from Nb or NbN alone. Even in this unfavorable field configuration, it is fairly higher than the reference sample, but only in the temperature range where niobium too is superconducting. These results will be detailed elsewhere, but they further support the effectiveness of the shielding of niobium in layered structures [32].

In our case we need to develop in addition an experimental setup where the field configuration is similar to cavities, i.e., parallel to the surface.

B. Depositing technique

We need to determine how the screening properties evolve in more realistic situations. We plan to test samples deposited on bulk monocrystalline and polycrystalline niobium with the same technique or with alternative techniques like atomic layer deposition (ALD), which might be easier to develop for full cavity deposition.

V. CONCLUSION

We have presented the superconducting properties of composite structures specifically designed for rf accelerating applications. In particular, we have analyzed SL and ML multilayer by dc SQUID magnetization measurement in a parallel field configuration. We have shown very promising behavior of these composite structures: the first critical field of a multilayer is strongly enhanced and the vortex penetration is prevented at fields higher than the niobium first penetration field when the field is parallel to the surface.

Moreover, when the field is applied locally, this effect seems to be also noticeable in the perpendicular field as shown by the 3rd harmonic analysis.

These results are encouraging for cavity application where the nonplanarity of the surface may induce some local small vertical field component. We must now optimize the number and thickness of layers necessary to reach the best shielding effect. Increasing the number of layers should indeed increase the shielding, but depending on the deposition technique, some degradation of the layers' quality with thickness is expected, and probably a compromise must be found in more realistic conditions. Various other superconducting materials should also be tested. We need to determine how the screening properties evolve in more realistic situations. We plan to test samples deposited on bulk monocrystalline and polycrystalline niobium with the same technique or with alternative techniques like ALD, which might be easier to develop for full cavity deposition. Ultimately rf cavities should be tested at 1.3 GHz. Recent results obtained on a 20 GHz Nb strip line resonator show that H_{C1} is indeed significantly increased in thin films under rf field [33].

ACKNOWLEDGMENTS

The research leading to these results has received partial funding from the European Commission under the FP7 Research Infrastructures project EuCARD, Grant Agreement No. 227579.

[1] P. Bauer *et al.*, Physica C (Amsterdam) **441**, 51 (2006).
[2] A. Gurevich, Physica C (Amsterdam) **441**, 38 (2006).
[3] http://conferences.jlab.org/tfsrf/Tuesday/Tu2_3-Trapped_vortices_Ciovati.pdf.
[4] http://tdserver1.fnal.gov/project/workshops/RF_Materials/talks/A-M_Valente-Feliciano_NewMaterialsOverview.ppt.
[5] A. Gurevich, Appl. Phys. Lett. **88**, 012511 (2006).
[6] http://conferences.jlab.org/tfsrf/ThinfilmWorkshop_Agenda.pdf.
[7] T. Proslier *et al.*, Appl. Phys. Lett. **93**, 192504 (2008).
[8] M.J. Pellin *et al.*, in SRF 2007, Beijing, China [http://cern.ch/AccelConf/srf2007/PAPERS/TUP64.pdf].
[9] J-C. Villegier *et al.*, IEEE Trans. Appl. Supercond. **19**, 3375 (2009).
[10] L.G. Parratt, Phys. Rev. **95**, 359 (1954).
[11] L. Civale *et al.*, Appl. Phys. Lett. **84**, 2121 (2004).
[12] D. Feinberg and C. Villard, Phys. Rev. Lett. **65**, 919 (1990).
[13] C. Monton, F. de La Cruz, and J. Guimpel, Phys. Rev. B **75**, 064508 (2007).
[14] F.M. Sauerzopf, H.P. Wiesinger, and H.W. Weber, Cryogenics **30**, 650 (1990).
[15] E.M. Gyorgy *et al.*, Appl. Phys. Lett. **55**, 283 (1989).
[16] S. Candia and L. Civale, Supercond. Sci. Technol. **12**, 192 (1999).
[17] J.R. Thompson *et al.*, Supercond. Sci. Technol. **23**, 014002 (2010).
[18] E. Zeldov *et al.*, Phys. Rev. B **49**, 9802 (1994).
[19] K. Li and Y. Zhang, J. Phys. Condens. Matter **7**, 9845 (1995) [http://iopscience.iop.org/0953-8984/7/50/018].
[20] L.E. De Long *et al.*, Physica C (Amsterdam) **468**, 523 (2008).
[21] S. Kryukov, W. Xu, and L. de Long, in American Physical Society March Meeting, 2007 [http://meetings.aps.org/Meeting/MAR07/Event/56477].
[22] A.A. Zhukov *et al.*, Phys. Rev. B **56**, 2809 (1997).

[23] Quantum Design MPMS Application Note No. 1014-202 A.
[24] C. Z. Antoine *et al.*, in SRF 2009, Berlin, Germany [http://accelconf.web.cern.ch/AccelConf/SRF2009/papers/tuppo070.pdf].
[25] V. V. Chabanenko *et al.*, J. Appl. Phys. **88**, 5875 (2000).
[26] A. Nabialek *et al.*, J. Low Temp. Phys. **139**, 239 (2005) [http://www.springerlink.com/content/t356t255867621v2].
[27] N. I. Balalykin and A. B. Kuznetsov, SRF 97, Abano Terme (Padova), Italy, 1997 [http://cern.ch/AccelConf/SRF97/papers/srf97b11.pdf].
[28] G. P. Mikitik, Low Temp. Phys. **36**, 13 (2010).
[29] R. Lortz *et al.*, Phys. Rev. B **75**, 094503 (2007).
[30] L. Krusin-Elbaum *et al.*, Phys. Rev. Lett. **69**, 2280 (1992).
[31] R. Russo *et al.*, IEEE Trans. Appl. Supercond. **19**, 1394 (2009).
[32] C.Z. Antoine, S. Berry, M. Aurino, J.F. Jacquot, J.C.Villegier, G. Lamura, and A. Andreone, ‘‘Characterization of field penetration in superconducting multilayers samples,’’ IEEE Trans. Appl. Supercond. (to be published).
[33] N. Groll, A. Gurevich, and I. Chiorescu, Phys. Rev. B **81**, 020504 (2010).